

EVALUATION OF SLIDING MODE OBSERVER FOR VEHICLE SIDESLIP ANGLE

Stéphane Joanny* Charara Ali*
Meizel Dominique**

* *HEUDIASYC Laboratory (UMR CNRS UTC 6599) -
Centre de recherche de Royallieu BP20529 - 60205
COMPIEGNE cedex France*

joanny.stephant@hds.utc.fr, ali.charara@hds.utc.fr

** *GERME - ENSIL - 16 rue Atlantis Parc d'Ester
Technopole BP 6804 - 87068 LIMOGES cedex France
meizel@ensil.unilim.fr*

Abstract: Vehicle sideslip angle is the principal variable used in computing the transversal forces governing tire/road contact. It is the most important variable determining a vehicle's lateral stability. This paper presents a sliding mode observer of vehicle sideslip angle. A model is developed and then simplified. The observer was tested on a validated simulator and on experimental data acquired using a real vehicle. A "Correxit" optical speed sensor was used to measure the sideslip angle. We discuss the limitations of using a nonlinear vehicle model with linear transversal forces. This paper also presents the relation between nonlinear observability and certain vehicle parameters. *Copyright ©2005 IFAC*

Keywords: Vehicle dynamics, Nonlinear systems, State observers, Observability

1. INTRODUCTION

A vehicle is a highly complex system bringing together a large number of mechanical, electronic and electromechanical elements. To describe all the movements of the vehicle, numerous measurements and a precise mathematical model are required.

In vehicle development, knowledge of wheel-ground contact forces is important. This information is useful for security actuators, for validating vehicle simulators and for advanced vehicle control systems.

Braking and control systems must be able to stabilize the car during cornering. When subject to transversal forces, such as when cornering, or in the presence of a camber angle, tire torsional flexibility produces an aligning torque which mod-

ifies the original wheel direction. The difference is characterized by an angle known as "sideslip angle". This is a significant signal in determining the stability of the vehicle (Bulteau *et al.*, 2002), and it is the main transversal force variable. Measuring sideslip angle would represent a disproportionate cost in the case of an ordinary car, and it must therefore be observed or estimated.

The aim of an observer or virtual sensor is to estimate a particular unmeasurable variable from available measurements and a system model. This is an algorithm which describes the movement of the unmeasurable variable by means of statistical conclusions from the measured inputs and outputs of the system. This algorithm is applicable only if the system is observable.

This paper presents methods which uses simple models and two measurements in order to estimate one particular unmeasurable variable: sideslip angle. The literature describes several observers for sideslip angle. For example, (Kiencke and Nielsen, 2000) presents linear and nonlinear observers using a bicycle model. (Venhovens and Naab, 1999) uses a Kalman filter for a linear vehicle model. (Stéphant *et al.*, 2003) presents a comparison of several linear and nonlinear observers. Performances obtained through simulation and experimentation using several classical pure lateral dynamics tests are presented, and the nonlinear observability problem and its relation to vehicle speed and cornering stiffness are discussed. Finally, we declare the domain of validity for this observer.

2. VEHICLE MODEL

Lateral vehicle dynamics has been studied since the 1950s. In 1956 Segel (Segel, 1956) presented a vehicle model with three degrees of freedom in order to describe lateral movements including roll and yaw. If roll movement is neglected, a simple model known as the "bicycle model" is obtained. This model is currently used for studies of lateral vehicle dynamics (yaw and sideslip). A nonlinear representation of the bicycle model is shown in Figure 1. Notations are explained in section 9. Certain simplifications are used in this study.

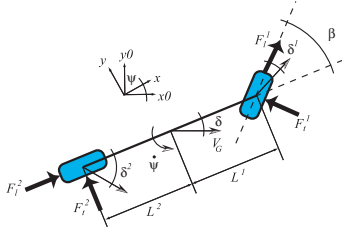


Fig. 1. Schematic representation of bicycle model

Cornering stiffness is taken to be constant. But cornering stiffness is modified with vertical forces on the wheel. Variations of cornering stiffness during the course of a double lane change are shown in figure 7.

Tire/road forces are highly nonlinear. Various wheel-ground contact force models are to be found in the literature, including a comparison between three different models in (Stéphant *et al.*, 2002). In this paper, transversal forces are taken to be linear. Consequently, transversal forces can be written as:

$$F_y^i = C_{F\delta}^i \cdot \delta^i \quad i = 1, 2 \quad (1)$$

Rear and front tire sideslip angles are calculated as:

$$\begin{cases} \delta^1 = \beta - \delta - L^1 \frac{\dot{\psi}}{V_G} \\ \delta^2 = -\delta + L^2 \frac{\dot{\psi}}{V_G} \end{cases} \quad (2)$$

The vehicle model can be expressed in terms of a nonlinear state space formulation as follows:

$$\dot{\mathbf{X}} = \mathbf{f}_{NL}(\mathbf{X}, \mathbf{U}) \quad (3)$$

With $\mathbf{X} = (V_G \ \delta \ \dot{\psi})^T$, $\mathbf{U} = (\beta \ F_l^1 \ F_l^2)^T$ and

$$\begin{cases} \dot{\mathbf{x}}_1 = \frac{1}{m_v} \mathbf{u}_2 \cos(\mathbf{x}_2 - \mathbf{u}_1) + \mathbf{u}_3 \cos(\mathbf{x}_2) \\ \quad + \frac{1}{m_v} C_{F\delta}^2 \left(-\mathbf{x}_2 + L^2 \frac{\mathbf{x}_3}{\mathbf{x}_1} \right) \sin(\mathbf{x}_2) \\ \quad + \frac{1}{m_v} C_{F\delta}^1 \left(\mathbf{u}_1 - \mathbf{x}_2 - L^1 \frac{\mathbf{x}_3}{\mathbf{x}_1} \right) \sin(\mathbf{x}_2 - \mathbf{u}_1) \\ \dot{\mathbf{x}}_2 = \frac{1}{m_v \mathbf{x}_1} \mathbf{u}_2 \sin(\mathbf{u}_1 - \mathbf{x}_2) - \mathbf{u}_3 \sin(\mathbf{x}_2) \\ \quad + \frac{1}{m_v \mathbf{x}_1} C_{F\delta}^1 \left(\mathbf{u}_1 - \mathbf{x}_2 - L^1 \frac{\mathbf{x}_3}{\mathbf{x}_1} \right) \cos(\mathbf{u}_1 - \mathbf{x}_2) \\ \quad + \frac{1}{m_v \mathbf{x}_1} C_{F\delta}^2 \left(-\mathbf{x}_2 + L^2 \frac{\mathbf{x}_3}{\mathbf{x}_1} \right) \cos(\mathbf{x}_2) - \mathbf{x}_3 \\ \dot{\mathbf{x}}_3 = \frac{1}{I_{zz}} \left(L^1 \mathbf{u}_2 \sin(\mathbf{u}_1) - L^2 C_{F\delta}^2 \left(-\mathbf{x}_2 + L^2 \frac{\mathbf{x}_3}{\mathbf{x}_1} \right) \right) \\ \quad + \frac{1}{I_{zz}} L^1 C_{F\delta}^1 \left(\mathbf{u}_1 - \mathbf{x}_2 - L^1 \frac{\mathbf{x}_3}{\mathbf{x}_1} \right) \cos(\mathbf{u}_1) \end{cases} \quad (4)$$

The state comprises the speed of center of gravity V_G , the sideslip angle δ and the yaw rate $\dot{\psi}$. Inputs are the front wheel steering angle β and the longitudinal forces applied to the front F_l^1 and rear F_l^2 wheels.

3. SLIDING MODE OBSERVER

From (Perruquetti and Barbot, 2002) it is clear that this kind of observer is useful when working with reduced observation error dynamics and when seeking a finite time convergence for all observable states, as well as robustness when confronted with parameter variations (with respect to conditions). Figure 2 presents the sliding mode observer method applied to a nonlinear vehicle model (3).

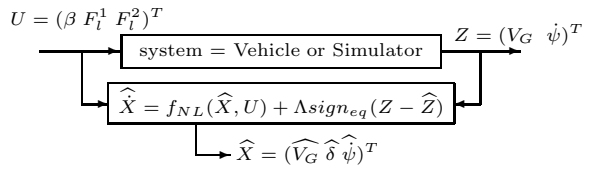


Fig. 2. Sliding mode observer method

In this paper two measurements are used to estimate the vehicle sideslip angle: the yaw rate and the speed of the center of gravity. The first measurement is available from the ESP control unit, and the second can be calculated from the ABS sensors. The observation equation can be written :

$$\begin{aligned} \mathbf{Z} &= \mathbf{h}_{NL}(\mathbf{X}) = (h_1(\mathbf{X}) \ h_2(\mathbf{X}))^T \\ &= (\mathbf{x}_1 \ \mathbf{x}_3)^T = (V_G \ \dot{\psi})^T \end{aligned} \quad (5)$$

The sliding mode observer equations are:

$$\begin{cases} \hat{\mathbf{X}} = \mathbf{f}_{NL}(\hat{\mathbf{X}}, \mathbf{U}) + \mathbf{\Lambda} \text{sign}_{eq}(\mathbf{Z} - \hat{\mathbf{Z}}) \\ \hat{\mathbf{Z}} = \mathbf{h}_{NL}(\hat{\mathbf{X}}) \end{cases} \quad (6)$$

where $\mathbf{\Lambda}$ is the observer gain matrix in $\mathbb{R}^{3 \times 2}$. To cover chattering effects (Chabraoui, 2001), the function sign_{eq} used in this paper is

$$\text{sign}_{eq}(x) = \arctan(x) * 2/\pi$$

4. OBSERVABILITY

Using the nonlinear state space formulation, the observability definition is local and uses the Lie derivative (Nijmeijer and Van der Schaft, 1990). It is a function of state trajectory and inputs applied to the model. For the system described by equation (6) and sensor set (5) the observability function is:

$$\mathbf{o}(\mathbf{X}, \mathbf{U}) = \begin{pmatrix} h_1(\mathbf{X}) \\ (\mathcal{L}_f h_1)(\mathbf{X}, \mathbf{U}) \\ (\mathcal{L}_f^2 h_1)(\mathbf{X}, \mathbf{U}) \\ h_2(\mathbf{X}) \\ (\mathcal{L}_f h_2)(\mathbf{X}, \mathbf{U}) \\ (\mathcal{L}_f^2 h_2)(\mathbf{X}, \mathbf{U}) \end{pmatrix} \quad (7)$$

with

$$\begin{aligned} \mathcal{L}_f h_j(\mathbf{X}) &= \frac{dh_j(\mathbf{x})}{d\mathbf{X}} \mathbf{f}_{NL}(\mathbf{X}, \mathbf{U}) \\ \mathcal{L}_f^{i+1} h_j(\mathbf{X}) &= \frac{d\mathcal{L}_f^i h_j(\mathbf{X})}{d\mathbf{X}} \mathbf{f}_{NL}(\mathbf{X}, \mathbf{U}) \end{aligned} \quad (8)$$

If the \mathbf{o} function is invertible at the current state and input, the system is observable. This function is invertible if its Jacobian matrix \mathbf{O} has a full rank.

$$\mathbf{O} = \frac{d}{d\mathbf{X}} \mathbf{o}(\mathbf{X}, \mathbf{U}) \quad (9)$$

It is also possible to give an observability indicator with the inverse of the Jacobian matrix condition number. This gives a measure of the sensitivity of the solution to the observation problem.

5. SIMULATION RESULTS

The Callas simulator provides simulations which can be used to study the performance of the sliding mode observer of vehicle sideslip angle. This software is a realistic simulator validated by car manufacturers and research institutions including INRETS ("Institut national de recherche sur les transports et leur sécurité"). The Callas model takes into account vertical dynamics (suspension, tires), kinematics, elasto-kinematics, tire adhesion and aerodynamics. This vehicle simulator was developed by SERA-CD (<http://www.sera-cd.com>).

Sideslip angle is the most important variable used when calculating tire/road transversal forces and

studying the lateral stability of a vehicle. The performance of the observer is evaluated on an ISO double lane change. This kind of test is representative of the transient lateral behavior of a vehicle. The double lane change is performed at three different speeds: 40km/h, 90km/h and 105km/h. The difference between the three tests is the level of lateral acceleration. At 105km/h the level is so high that the simulator's virtual driver lost control of the car.

5.1 Observer results

Figure 4 presents results of the reconstruction of vehicle sideslip angle by the sliding mode observer (6). Figure 3 summarizes the performance of the observer in estimating different variables.

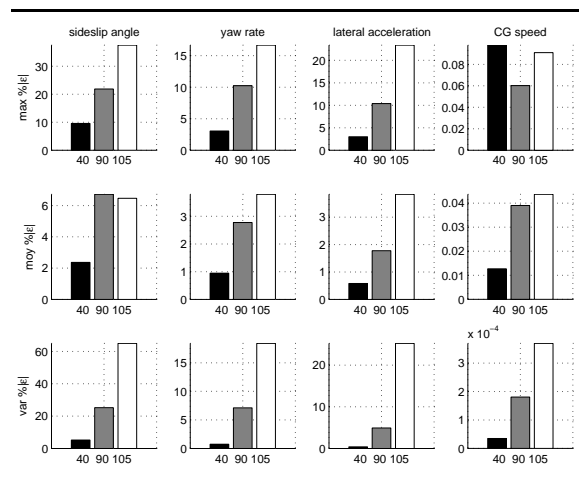


Fig. 3. Normalized error by the observer for an ISO double lane change at 40km/h, 90km/h and 105km/h. Error on sideslip angle, yaw rate, lateral acceleration and vehicle speed

The three rows of histograms present the normalized error attributable to the observer. The normalized error of a variable z is defined by :

$$\epsilon_z = \frac{|z_{SMO} - z_{Callas}|}{\max(|z|)} \quad (10)$$

where z_{SMO} is the variable calculated by the observer, z_{Callas} is the variable calculated by the Callas simulator and $\max(|z|)$ is the absolute maximum value of the variable during the test maneuver.

The first row shows the maximum normalized error during the course of the maneuver. The second row shows the mean, and the third row the variance. The first column on the left presents the results for sideslip angle observation, the second column the yaw rate estimation, the third the lateral acceleration, and the rightmost column the vehicle speed. The black, gray and white blocks represent the maneuver at 40km/h, 90km/h and 105km/h respectively.

The lateral acceleration is calculated by:

$$\hat{y} = \left(\frac{C_{F\delta}^1}{m_v} \right) \beta + \left(\frac{C_{F\delta}^2 L^2 - C_{F\delta}^1 L^1}{m_v \hat{V}_G} \right) \hat{\psi} + \left(-\frac{C_{F\delta}^1 + C_{F\delta}^2}{m_v} \right) \hat{\delta} \quad (11)$$

where variables are estimated by the sliding mode observer.

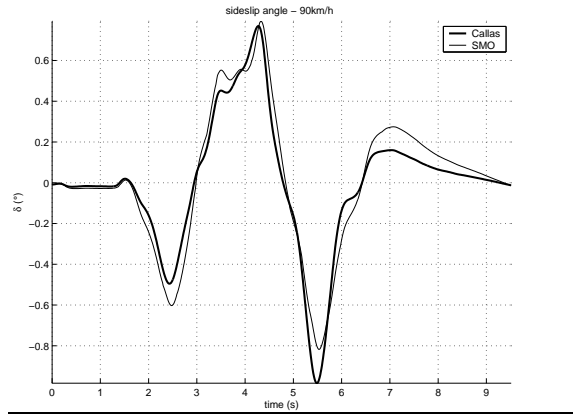


Fig. 4. Sideslip angle by sliding mode observer for an ISO double lane change at 90km/h

As shown in the last column of figure 3, the vehicle speed is calculated precisely by the sliding mode observer. All the variables are correctly estimated for the maneuver at 40km/h. On average the sideslip angle error is around 2%, the yaw rate error 1% and the lateral acceleration error 0.5%. As regards the different lateral variables, the higher the speed, the greater the maximum normalized error, and the greater the error variance. The same applies to yaw rate and to lateral acceleration. The level of error is around 6.5% for the sideslip angle estimation at 90 and 105km/h. It should be noted that for this kind of path, the speed is directly linked to the lateral force applied.

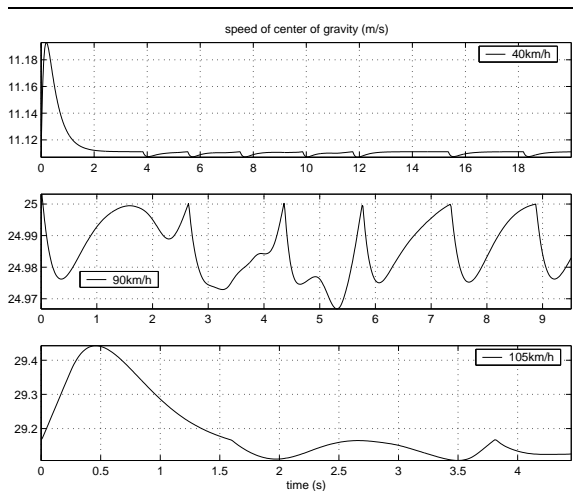


Fig. 5. Vehicle speed for an ISO double lane change at 40km/h, 90km/h and 105km/h

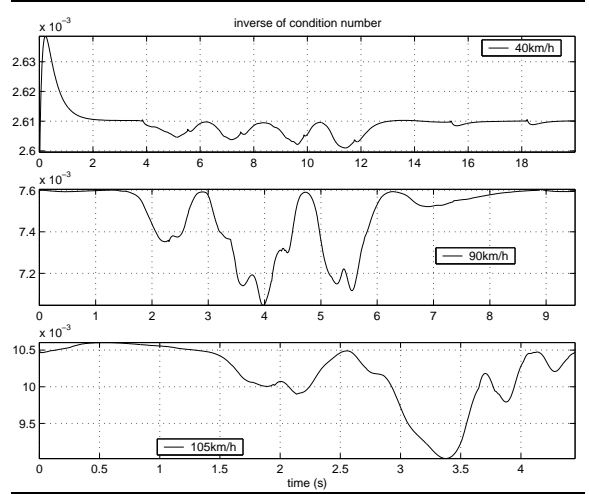


Fig. 6. Inverse of condition number of observability matrix for the sliding mode observer and the three ISO double lane changes

5.2 Observability results

The rank of the observability matrix (9) is 3 along the three different paths. The model is observable.

Figure 6 presents the inverse of condition number of matrix \mathbf{O} . Two conclusions may be drawn about this property of the observability matrix. First, the greater the speed, the smaller the condition number. At 40km/h, the condition number is around 380, at 90km/h 135 and at 105km/h 100. The shape of the condition number is related to the shape of vehicle speed shown in figure 5.

The second conclusion can be drawn by comparing the shape of the tire cornering stiffness, shown in figure 7, with the shape of the condition number of the observability matrix. The greater the variation in real cornering stiffness, the greater the condition number of the observability matrix.

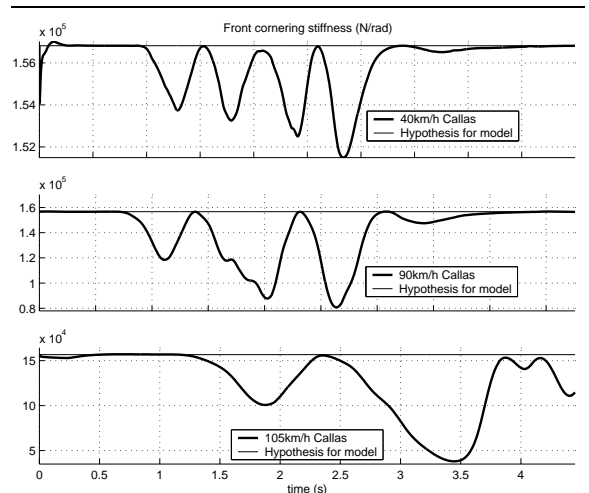


Fig. 7. Front cornering stiffness for an ISO double lane change at 40km/h, 90km/h and 105km/h. Simulator calculation and hypothesis used for observer construction

6. EXPERIMENTAL RESULTS

In order to study experimentally the performance of the vehicle sideslip angle sliding mode observer, data were collected using the Heudiasyc laboratory vehicle (to be presented in the following section.) The test was a slalom performed at high speed (80km/h). As long as the car is being controlled by a driver, the steering angle amplitude and frequency are increasing. With this kind of path, the lateral pressure applied depends on the steering input. The first aim of this test was to determine the level of lateral pressure at which the results yielded by the sliding mode observer become too high. The second aim was to confirm our conclusion regarding the properties of the observability matrix.

6.1 Experimental vehicle

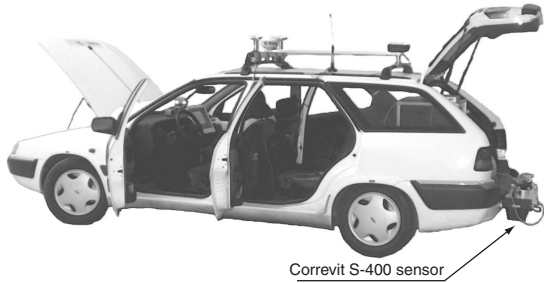


Fig. 8. STRADA: Heudiasyc laboratory experimental vehicle

STRADA is the Heudiasyc Laboratory's test vehicle: a Citroën Xantia station wagon equipped with number of sensors, shown in figure 8. Tests described in this paper use

- Lateral accelerometer
- Odometry: rotation speeds of the four wheels (ABS sensors)
- Yaw rate gyrometer
- Steering angle
- Correvit Sensor

The speed of the center of gravity is calculated as the mean of the longitudinal speeds of the two rear wheels (odometry).

The Correvit S-400 is a noncontact optical sensor mounted at the rear of STRADA on the sprung mass of the car. The S-400 Sensor provides highly accurate measurement of distance, speed and acceleration, sideslip angle, drift angle and yaw angle. The S-400 Sensor uses proven optical correlation technology to ensure the most accurate possible signal representation. This technology incorporates a high intensity light source that illuminates the test surface, which is optically detected by the sensor via a two-phase optical grating system.

6.2 Observer results

Figure 9 presents the estimation of sideslip angle using the sliding mode observer (6) and the vehicle's lateral acceleration.

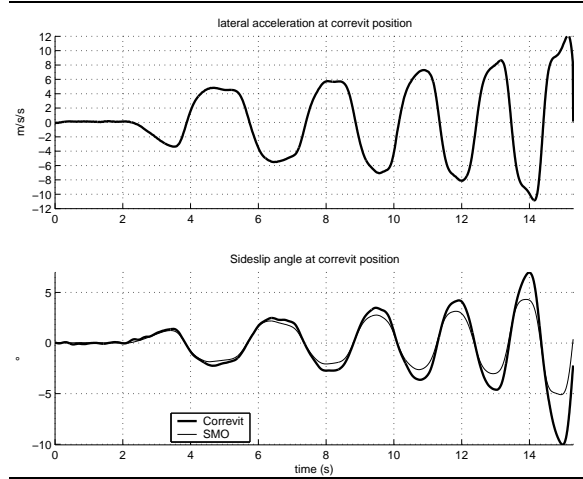


Fig. 9. Measured lateral acceleration and sideslip angle, sideslip angle estimated by sliding mode observer

It was shown that the linear approximation for tire/road transversal forces is valid when the lateral acceleration does not exceed 0.4g, and that a linear vehicle bicycle model is representative when the lateral acceleration does not exceed 0.3g (Lechner, 2001). In this model we assume that cornering is performed at constant speed. The speed over the slalom test was approximately constant at 80km/h, as shown in the upper part of figure 10. Given these conditions, the nonlinear model (3) shows the same characteristics as the linear bicycle model.

From figure 9 it can be seen that the error in sideslip angle estimation attributable to the sliding mode observer is less than 0.5° until 6.8 seconds have elapsed, and then 1° between 6.8 and 12.5 seconds. Subsequently the error increases. On the three last peaks the error is 1.7, 2.8 and 5° . This error level can be linked to the lateral acceleration. Between 0 and 6.8 seconds the lateral acceleration remains less than 0.57g at peak values. Between 6.8 and 12.5 seconds lateral acceleration is between 0.6 and 0.8g. After 12.5 seconds lateral acceleration exceeds 0.8g at peak values, which means that the observer can no longer estimate the sideslip angle correctly.

If a vehicle sideslip angle error of less than 0.5° is acceptable, then it is possible to use the observer presented in this paper when lateral acceleration does not exceed 0.6g. However, when the lateral acceleration exceeds 0.6g, this observer is not sufficiently accurate.

The rank of the observability matrix is 3 throughout the slalom test. Using this criterion, the model is observable. Figure 10 presents the inverse of observability condition number. As we have shown in relation to the validation by simulation, the condition number is directly linked to the real cornering stiffness. In actual slalom tests the resulting cornering stiffness (by axle) decreases with each cornering. The decreasing peaks of the condition number curve correspond to the peaks of the vehicle sideslip angle curve. The greater the sideslip angle estimation error, the higher the condition number.

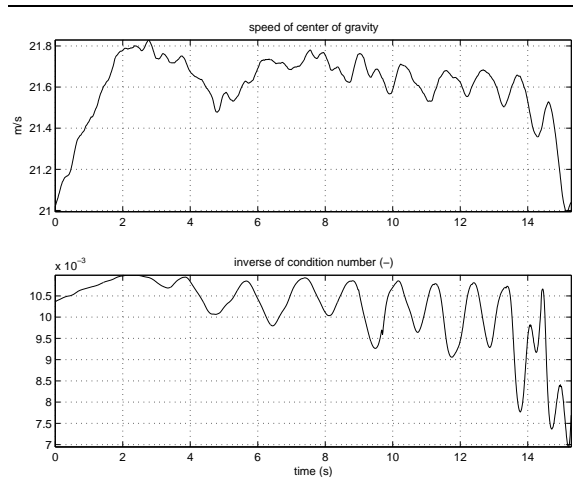


Fig. 10. Speed of vehicle and inverse of observability matrix condition number

7. CONCLUSION

This paper has presented in detail the properties of a vehicle sideslip angle sliding mode observer applied to a nonlinear bicycle vehicle model. The first conclusion is that with a lateral acceleration not exceeding 0.6g, observer results are quite good. The second conclusion is that the condition number of the observability matrix provides an indicator regarding the quality of the estimation. Since the condition number is directly related to the variations in speed and cornering stiffness, the speed being known, it would appear possible to identify the real cornering stiffness from the calculation of this condition number.

8. ACKNOWLEDGMENTS

This study was carried out in partnership with the "Diagnostic et Véhicules Avancés" research group, financed by the Picardie region, and within the framework of the "Action de Recherche pour une CONduite sécurisée" project, financed by the PREDIT program.

- $C_{F\delta}^{1,2}$ Front, rear wheel cornering stiffness ($N.rad^{-1}$)
- $F_l^{1,2}$ Longitudinal force in the front, rear wheel frame (N)
- $F_t^{1,2}$ Transversal force in the front, rear wheel frame (N)
- $L^{1,2}$ CG to front, rear axle distance (m)
- V_G Speed of center of gravity ($m.s^{-1}$)
- β Steering angle (rad)
- δ Vehicle sideslip angle (rad)
- $\delta^{1,2}$ Front, rear wheel sideslip angle (rad)
- $\dot{\psi}$ Yaw rate ($rad.s^{-1}$)

REFERENCES

- Bulteau, Francois, Jacques Sainte-Marie, Said Mammam and Sébastien Glaser (2002). "modèle non linéaire des véhicules et étude des situations en limite de stabilité". *Proc. CIFA 2002, Nantes, France*.
- Chabraoui, S (2001). "observateurs à modes glissants dédiés aux systèmes possédant des singularités d'observation". *Journées Doctorales d'Automatique, Toulouse, France*.
- Kiencke, Uwe and Lars Nielsen (2000). "Automotive control system". Springer.
- Lechner, Daniel (2001). "Analyse du comportement dynamique des véhicules routiers légers : développement d'une méthodologie appliquée à la sécurité primaire". PhD thesis. École centrale de Lyon.
- Nijmeijer, H and A. J. Van der Schaft (1990). *Nonlinear Dynamical Control Systems*. Springer-Verlag.
- Perruquetti, Wilfrid and Jean-Pierre Barbot (2002). *Sliding mode control in engineering*. Marcel Dekker, Inc.
- Segel, M.L. (1956). "theoretical prediction and experimental substantiation of the response of the automobile to steering control". *Proc. automobile division of the institut of mechanical engineers*.
- Stéphant, Joanny, Ali Charara and Dominique Meizel (2002). "force model comparison on the wheel-ground contact for vehicle dynamics". *Proc. IEEE Intelligent Vehicle Symposium - Versailles*.
- Stéphant, Joanny, Ali Charara and Dominique Meizel (2003). "vehicle sideslip angle observers". *Proc. European Control Conference (ECC2003), Cambridge, U.K.*
- Venhovens, P.J.TH and Karl Naab (1999). "vehicle dynamics estimation using kalman filters". *Vehicle System Dynamics* **32**, 171-184.